SRC TR 88-80

Reduction Of A Structured Model To An Equivalent Unstructured Model

by

N.S. Wang and G. Stephanopoulos

REDUCTION OF A STRUCTURED MODEL TO AN EQUIVALENT UNSTRUCTURED MODEL

by

Nam Sun Wang
Department of Chemical and Nuclear Engineering
University of Maryland
College Park, MD 20742-2105, U.S.A.
and
Gregory Stephanopoulos
Department of Chemical Engineering
Massachusetts Institute of Technology
Cambridge, MA 02139, U.S.A.

Presented at
Fourth International Congress
on Computer Applications
in Fermentation Technology:
Modelling and Control of
Biotechnical Processes
University of Cambridge, UK
September 25-29, 1988

ABSTRACT

A new modeling approach that employs a time-lag kernel can be used to transform a complicated structured model to an equivalent unstructured model. It can be shown that the connection between the two types of models is provided by the time-lag kernel, as a natural consequence of reducing a larger set of dynamic equations of a structured model to a smaller set of dynamic equations of an unstructured model. The time-lag kernel compacts the process of a cell's response to the external stimuli into a simple functional form. This modeling approach retains the general form of an unstructured model so as to facilitate simple physical interpretation of the variables. Yet, it retains the predictive power of a structured model by incorporating only those metabolic intermediates that are important to the dynamics of the system. The order of a structured model is reduced through the judicious process of lumping and modal analysis of the eigenvalue-eigenvector of a quasi-linearized system. By identifying the first few most important modes, such an analysis yields useful information on the relative time scales of various processes and clarifies the main feature of the model. The application of the approach is demonstrated with different structured models. Since a model is to be judged based on its intended purpose, in many applications a time-lag kernel approach is a viable, attractive alternative to either an oversimplified unstructured model that does not perform adequately, an overly complex structured model whose detailed description is unnecessary, or a purely black box approach that has little appeal due to the total lack of process structures. The use of the time-lag model in the fermentation control's environment will be discussed.

INTRODUCTION

This study is motivated by the general observation that time-lag effects frequently exist in a biochemical reactor system. Its existence has long been recognized, for example, at the beginning of a batch fermentation in the form of a lag phase. It is also present when a culture is transferred into a new richer medium that is capable of supporting a higher growth rate than the original one. The recognition of the inadequacy of the unstructured models in predicting the lag behavior has prompted the proposal of a range of structured models to explain these time-lag observations. However, most of these models are too complicated and are unsuitable for process control purposes.

The objective of this study is to develop a simple model that can predict a variety of transient as well as steady-state behaviors commonly encountered in a biological reactor. Some of these behaviors include lag phases, diauxic growth, asymmetric responses, hysteresis effects, and damped and sustained oscillations. The model shall express the cause-effect relationship in a form appropriate for practical use in a process design and control environment.

In this paper, a new approach to bioprocess identification and modeling is outlined. The proposed approach considers the effect on rates and yields of not only the present state of the system but also the previous history through the concept of a kernel integral. The resulting set of integro-differential equations are then shown to be equivalent to a set of first-order ordinary differential equations representing a generalized structured model. These simple ordinary differential equations can then be relatively easily manipulated with the well developed mathematical techniques to yield insightful information on the dynamics of the system, including the analysis of the stability of steady states, etc. Furthermore, size reduction techniques are outlined, which can lead to a directly observable model of a lower dimension while

preserving simultaneously the biological significance of various parameters. Finally, it is demonstrated experimentally that a time-lag model can be used to predict correctly transient behaviors based on parameters that have been determined from steady-state fermentation runs. The experiments were conducted in accordance with the state-of-the-art on-line monitoring techniques, and on-line and off-line data were analyzed with advanced parameter estimation algorithms.

FORMULATION OF TIME-LAG MODEL

Time-lag effects are frequently encountered in microbial systems. For example, they are present at the beginning of a batch fermentation in the form of a lag phase. When the nutrient concentration is increased, the level of growth enzymes present in a cell must be increased before a higher rate of biomass synthesis can be achieved. Again, the metabolic mechanism in this case must be adjusted, and a factory with a higher capacity has to be assembled so that a larger amount of chemicals can flow through the anabolic and catabolic pathways. For example, when the limiting substrate concentration is increased as a result of a step change in the dilution rate in a continuous fermentor, the specific growth rate of the microorganism does not start to increase immediately, as does the limiting substrate concentration. In addition to the aforementioned time-lag phenomena, time-lag effects are also manifested in various observed oscillatory behaviors due to the response's dependence on the past history. It is well known that time-lags in control variables can destabilize a system and render it oscillatory. Similarly, the presence of time-lags in state variables can also profoundly influence the stability of the system and cause an otherwise stable system to oscillate. Oscillations in biological systems are quite prevalent and are frequently reported in literature.

In this section, we will formulate a model using the time-lag kernel approach and answer questions regarding the kernel's functional form. The essence of the

approach is the inclusion of kernel functions in the equations that describes the dynamics of a bioreactor.

As an introductory example, first consider the familiar case of a continuous bioreactor modeled by a lumped-parameter two-state-variable model, namely:

$$\frac{dx(t)}{dt} = -Dx(t) + \mu(s)x(t) \tag{.1}$$

$$\frac{ds(t)}{dt} = D\left[s_f - s(t)\right] - \frac{1}{Y_s}\mu(s)x(t), \tag{.2}$$

where we assume that the specific growth rate, μ, of biomass, x, is a function of the limiting substrate, s.

In this paper, we will restrict our attention to the lag associated with cell growth. This lag can be incorporated into the above model with the introduction of a time-lag kernel, $k(t,h)$, in the specific growth rate:

$$\frac{dx(t)}{dt} = -Dx(t) + \left[\int_{-\infty}^{t} \mu[s(h)]k(t,h)dh\right] x \tag{.3}$$

$$\frac{ds(t)}{dt} = D\left[s_f - s(t)\right] - \frac{1}{Y_s}\left[\int_{-\infty}^{t} \mu[s(h)]k(t,h)dh\right] x(t). \tag{.4}$$

Note that in this formulation, the microorganism's growth rate is assumed to be affected by the chemical environment, namely the limiting substrate concentration in the fermentation broth surrounding a cell. Lag effects due to other environmental factors such as temperature, pressure, pH, ionic strength, and nutrient composition can also be handled similarly.

A general function $k(t)$ can be specified with a small number of coefficients such as a_0, a_1, etc, if it is expressed in terms of a series of base functions that belong to exponential distribution functions.

$$k(t) = a_0k_0(t) + a_1k_1(t) + a_2k_2(t) + \ldots + a_mk_m(t), \tag{.5}$$

where the general expression for the nth exponential distribution function is:

$$k_n(t) = \begin{cases} \frac{1}{Tn!}\left(\frac{t}{T}\right)^n e^{-\frac{t}{T}} & \text{for } t \geq 0 \\ 0 & \text{for } t < 0. \end{cases} \tag{.6}$$

The reason for choosing this relatively unknown set of exponential distribution functions is that they permit the transformation of the integro-differential equations into a set of simple first-order equations to be carried out with care. The first two exponential distribution functions are sometimes used in ecological studies of population dynamics, and they have over the years earned special names. The 0th-order exponential distribution function, $k_0(t)$, and the 1st-order exponential distribution function, $k_1(y)$, are called *weak* and *strong* generic delay, respectively.

$$\text{n=0} \qquad k_0 = \tfrac{1}{T}e^{-\frac{t}{T}} \quad \ldots \text{ weak generic delay} \tag{.7}$$

$$\text{n=1} \qquad k_1 = \tfrac{t}{T^2}e^{-\frac{t}{T}} \quad \ldots \text{ strong generic delay.} \tag{.8}$$

An interesting property of the exponential distribution function can be derived by differentiating Equation (.6) with respect to t:

$$\begin{aligned} T\frac{dk_n(t)}{dt} &= \frac{1}{T(n-1)!}\left(\frac{t}{T}\right)^{n-1}e^{-\frac{t}{T}} - \frac{1}{Tn!}\left(\frac{t}{T}\right)^n e^{-\frac{t}{T}} \\ &= k_{n-1}(t) - k_n(t). \end{aligned} \tag{.9}$$

Thus, the additional property is that:

$$T\frac{dk_n(t)}{dt} + k_n(t) = k_{n-1}(t) \quad \text{for } n = 0, 1, 2, \ldots, \tag{.10}$$

where

$$k_{-1}(t) = \delta(t) = \begin{cases} 0 & \text{for } t < 0 \\ \infty & \text{for } t = 0 \\ 0 & \text{for } t > 0. \end{cases} \tag{.11}$$

The above equation can also be regarded as a generating function for $k_n(t)$.

Accordingly, if $k(t)$ is expressed as the sum of m exponential distribution functions, the observed specific growth rate at time t, expressed as a functional $y(t) \equiv \int_{-\infty}^{t} \mu[s(h)]k(t-h)dh$, will be the weighed sum of m integrals, each of which

being $y_j(t) \equiv \int_{-\infty}^{t} \mu[s(h)]k_j(t-h)dh$ $j = 1, 2, ..., m$. This argument can be shown to be true by the following equation, starting with $k(t) = \sum_{j=0}^{m} a_j k_j(t)$:

$$\begin{aligned} y(t) &= \int_{-\infty}^{t} \mu[s(h)]k(t-h)dh \\ &= \int_{-\infty}^{t} \mu[s(h)] \overbrace{\left[\sum_{j=0}^{m} a_j k_j(t-h)\right]}^{k(t-h)} dh \\ &= \sum_{j=0}^{m} a_j \underbrace{\left[\int_{-\infty}^{t} \mu[s(h)]k_j(t-h)dh\right]}_{y_j(t)} \\ &= \sum_{j=0}^{m} a_j y_j(t). \end{aligned} \tag{.12}$$

In actuality, the weighing factors a_j's and the lag time-constant T are chosen in such a way as to fit the observed transient of the specific system in a shift-up or shift-down experiment. A small value of m varying from one to three usually gives a very satisfactory fit, and it is rarely necessary to employ m with orders larger than four.

The reason for choosing exponential probability distribution functions is that they permit the easy and elegant transformation of a set of integro-differential equations into a set of simple ordinary differential equations. These exponential distribution functions possess the property that each and every one of them is the solution to the following differential equation:

$$\boxed{\sum_{i=0}^{n+1} \binom{n+1}{i} T^i \frac{d^i k_n(t)}{dt^i} = 0}, \tag{.13}$$

with the initial conditions:

$$\frac{d^i k_n(0)}{dt^i} = 0 \qquad \text{for } i = 0, 1, 2, \ldots, n-1 \tag{.14}$$

$$\frac{d^n k_n(0)}{dt^n} = \frac{1}{T^{n+1}} \qquad \text{for } i = n. \tag{.15}$$

For example, $k_0(t) = \frac{t}{T}e^{-\frac{t}{T}}$ satisfies:

$$T\frac{dk_0(t)}{dt} + k_0(t) = 0 \tag{.16}$$

with the initial condition:

$$k_0(0) = \frac{1}{T}. \tag{.17}$$

Similarly, $k_1(t) = \frac{t}{T^2}e^{-\frac{t}{T}}$ satisfies:

$$T^2\frac{d^2k_1(t)}{dt^2} + 2T\frac{dk_1(t)}{dt} + k_1(t) = 0 \tag{.18}$$

with the set of initial conditions:

$$k_1(0) = 0 \tag{.19}$$

$$\frac{dk_1(0)}{dt} = \frac{1}{T^2}. \tag{.20}$$

The above properties of the exponential distribution functions can be used to eliminate the kernel from the integro-differential Equations (3) and (4) and convert them into a larger, but mathematically identical, set of first-order ordinary differential equations.

If we treat the integral containing the kernel as a new function $y_n(t)$, defined as:

$$y_n(t) \equiv \int_{-\infty}^{t} \mu(h)k_n(t-h)dh, \tag{.21}$$

then repeatedly differentiating $y_n(t)$ with respect to t with the help of Leibnitz's rule yields:

$$\boxed{\sum_{i=0}^{n+1}\binom{n+1}{i}T^i\frac{d^iy_n(t)}{dt^i} = \mu(t)}. \tag{.22}$$

In general, the resulting equivalent differential equation is one order higher than the kernel originally contained inside the integral in Equation (.21), including Equation (.22), which is the result of a special case of repeated roots for the

characteristic equation. For example, for the 0th-order kernel $k_0(t)$, the equivalent differential equation is:

$$T\frac{dy_0(t)}{dt} + y_0(t) = \mu(t). \tag{.23.0}$$

Similarly, for $n = 1$, $n = 2$, ..., $n - 1$, and n, the integrals involving $k_1(t)$, $k_2(t)$, ..., $k_{n-1}(t)$, and $k_n(t)$ are transformed respectively to:

$$T^2\frac{d^2y_1(t)}{dt^2} + 2T\frac{dy_1(t)}{dt} + y_1(t) = \mu(t) \tag{.23.1}$$

$$T^3\frac{d^3y_2(t)}{dt^3} + 3T^2\frac{d^2y_2(t)}{dt^2} + 3T\frac{dy_2(t)}{dt} + y_2(t) = \mu(t) \tag{.23.2}$$

$$\vdots \tag{.23}$$

$$T^n\frac{d^ny_{n-1}(t)}{dt^n} + nT^{n-1}\frac{d^{n-1}y_{n-1}(t)}{dt^{n-1}} + \ldots + nT\frac{dy_{n-1}(t)}{dt} + y_{n-1}(t) = \mu(t) \tag{.23.n - 1}$$

$$T^{n+1}\frac{d^{n+1}y_n(t)}{dt^{n+1}} + (n+1)T^n\frac{d^ny_n(t)}{dt^n} + \ldots + (n+1)T\frac{dy_n(t)}{dt} + y_n(t) = \mu(t). \tag{.23.n}$$

Notice the similarity between these equations, (*e.g.*, Equations (.23.0), (.23.1), and (.22)), and those equations that are satisfied by the corresponding kernel functions, (*e.g.*, Equations (.16), (.18), and (.13)). A higher-order differential equation such as Equation (.23.0) can be easily transformed into a set of first-order differential equations through some well known canonical transformations. Thus, for a 0th-order kernel, the set of integral state equations of (3) and (4) is reduced to the following:

$$\frac{dx}{dt} = (y - 1)x \tag{.24}$$

$$\frac{ds}{dt} = 1 - s - \frac{1}{Y_s}yx \tag{.25}$$

$$\frac{dy}{dt} = \frac{1}{T}(-y + \mu). \tag{.36}$$

As shown later, the biological significance of the 0th-order kernel can be extracted from the above equivalent set of equations. One of the possible interpretations of the above set of equations is that the rate of reproduction of the biomass is

autocatalytically proportional to the biomass itself and to a new variable y. If one so wishes, this variable y can be interpreted as the concentration or level of some "critical enzyme" that limits the growth of the microorganism. Furthermore, Equation (.26) indicates that this "critical enzyme" follows a first-order deactivation kinetics, and its rate of formation is described by the function $\mu(s)$. If μ has a Monod form, then the production of the enzyme follows that of Michaelis-Menton kinetics, which, incidentally, is originally derived to describe enzyme kinetics. Thus, time-lag formulation can partially explain the relationship between the enzyme kinetics and microbial specific growth rate in terms of the equivalence of the integral form and the differential form.

REDUCTION OF STRUCTURED MODELS TO UNSTRUCTURED MODELS

The difference between a complex structured model and a simple unstructured model is analogous to that between statistical and classical thermodynamics. Whereas a structured model attempts to explain the observed phenomena through a large set of differential equations in terms of the more fundamental variables such as the concentrations of various intermediates, unstructured models are usually composed of those variables that can be physically "seen" or "felt" more readily and are, thus, more comprehensible to human minds. The proposed modeling approach herein attempts to retain the general form of an unstructured model so as to facilitate simple physical interpretation of the variables by such familiar terms or concepts as the specific growth rate. At the same time, this modeling approach attempts to incorporate only those metabolic intermediates that are important to the dynamics of the system. It also attempts to reduce the order of a complicated structured model through the judicious process of lumping and the analysis

of eigenvalue-eigenvector of a linearized system. How this can be accomplished is outlined below.

Origin of the Time-Lag Kernel: In general, a dynamic system (including a structured model) can be described by a set of first-order differential equations:

$$\frac{d\mathbf{x}(t)}{dt} = \mathbf{f}(\mathbf{x}, \mathbf{u}, t), \tag{.27}$$

where $\mathbf{x}$ is the state vector and $\mathbf{u}$ is the input to the system. Currently, there is no general established way of solving such a set of differential equations if they are non-linear. As long as the nonlinearity is not too severe, one generally quasi-linearizes the nonlinear set of equations around the point of interest before attempting to solve them. For a system linear in the state variables, the above equation can be written as:

$$\frac{d\mathbf{x}(t)}{dt} = \mathbf{A}(t)\mathbf{x}(t) + \mathbf{g}(t). \tag{.28}$$

Note that the dependence of $\mathbf{A}$ on time does not destroy the linearity. The fundamental-matrix solution to the above differential equation is expressed by the following Lagrange formula:

$$\begin{aligned} \mathbf{x}(t) &= \int_{-\infty}^{t} \mathbf{K}(t,h)\mathbf{g}(h)dh \\ &= \mathbf{K}(t,t_0)\mathbf{x}(t_0) + \int_{t_0}^{t} \mathbf{K}(t,h)\mathbf{g}(h)dh, \end{aligned} \tag{.29}$$

where $\mathbf{K}$ is the fundamental matrix of Equation (.27).

$\mathbf{K}$ is also sometimes called the *transition matrix*. It has a few well known, extremely useful properties. The first one is that it satisfies the following matrix differential equation analogous to the homogeneous form of the state vector differential equation:

$$\frac{d\mathbf{K}(t,t_0)}{dt} = \mathbf{A}(t)\mathbf{K}(t,t_0) \qquad \text{for } t \geq t_0, \tag{.30}$$

with the initial condition:

$$\mathbf{K}(t_0, t_0) = \mathbf{I}. \tag{.31}$$

This dynamic relationship can be further generalized for any $h \geq t_0$:

$$\frac{d\mathbf{K}(t,h)}{dt} = \mathbf{A}(t)\mathbf{K}(t,h) \qquad \text{for } t \geq t_0, h \geq t_0. \tag{.32}$$

$$\mathbf{K}(h,h) = \mathbf{I} \qquad \text{for } h \geq t_0 \tag{.33}$$

The kernel matrix also satisfies the adjoint differential equation:

$$\frac{d\mathbf{K}^T(t,h)}{dh} = -\mathbf{A}^T(h)\mathbf{K}^T(t,h) \qquad \text{for } t \geq t_0, h \geq t_0. \tag{.34}$$

For any t_1, t_2, $t_3 \geq t_0$, the kernel matrix can be chained:

$$\mathbf{K}(t_3, t_1) = \mathbf{K}(t_3, t_2) \cdot \mathbf{K}(t_2, t_1). \tag{.35}$$

The above equation leads directly to the following identities:

$$\begin{aligned} \mathbf{I} = \mathbf{K}(t_1, t_1) &= \mathbf{K}(t_1, t_2) \cdot \mathbf{K}(t_2, t_1) \\ \Longrightarrow \mathbf{K}(t_1, t_2) &= \Big[\mathbf{K}(t_2, t_1)\Big]^{-1}. \end{aligned} \tag{.36}$$

Thus, the kernel matrix is nonsingular for all $t \geq t_0$ and $h \geq t_0$. This can also be seen from the fact that exponential functions are never equal to zero. Furthermore,

$$\det\Big|\mathbf{K}(t_2, t_1)\Big| = \exp\left\{\int_{t_1}^{t_2} \mathrm{tr}\Big[F(t)\Big]\right\} \tag{.37}$$

These properties are listed because they can be quite useful when handling a time-lag kernel.

Because the matrix $\mathbf{K}(t,h)$ depends on t and h separately and because the matrix itself may be monstrously dimensioned with numerous nonzero off-diagonal elements, it is difficult to be graphed and visualized in the traditional three-dimensional space that one is accustomed to. Thus, the meaning of each element of the matrix usually cannot be readily communicated with such conventional and easily comprehensible biochemical engineering terms as specific growth rate or yield, etc.

If the linearization matrix $\mathbf{A}(t)$ is constant, then this solution further reduces to:

$$\mathbf{x}(t) = \int_{-\infty}^{t} \mathbf{K}(t-h)\mathbf{g}(h)dh, \tag{.38}$$

where

$$\mathbf{K}(t) = e^{\mathbf{A}t}. \tag{.39}$$

Thus, the appearance of a kernel in Equations (3)-(4) is spontaneous; it arises mathematically during the process of solving a set of differential equations. As shown in the above derivation, what is called the kernel is mathematically equivalent to the fundamental matrix of a set of first-order ordinary differential equations. One also sees that the kernel inside the time-lag integral when expressed as $k(t-h)$ is actually the linearized time-invariant scalar representation of the more general form of $\mathbf{K}(t,h)$ of Equation (.29).

Time-Lag Kernel from a Structured Model: The structured model and the unstructured model are related in that a structured model can be reduced to an equivalent unstructured model. It will be shown that the connection between them is provided by the time-lag kernel.

The first step is to partition the vector of state variables, $\mathbf{x}(t)$, based on whether they appear in an unstructured model. Those variables that appear in the resulting unstructured model are grouped in $\mathbf{x}_1(t)$, and the remainder of the state vector $\mathbf{x}(t)$ that are included *only* in the structured model but not in the unstructured model are grouped in $\mathbf{x}_2(t)$. For example, the biomass, substrate, and product concentrations will be contained in $\mathbf{x}_1(t)$. All the intermediates and enzymes that are not considered as the product will be part of $\mathbf{x}_2(t)$. The result of this partition of $\mathbf{x}(t)$ is:

$$\mathbf{x}(t) = \begin{bmatrix} \mathbf{x}_1(t) \\ \mathbf{x}_2(t) \end{bmatrix}. \tag{.40}$$

The linearization matrix $\mathbf{A}(t)$ and the non-homogeneous forcing function $\mathbf{g}(t)$ can be partitioned similarly:

$$\mathbf{A}(t) = \begin{bmatrix} \mathbf{A}_{11}(t) & \mathbf{A}_{12}(t) \\ \mathbf{A}_{21}(t) & \mathbf{A}_{22}(t) \end{bmatrix} \tag{.41}$$

$$\mathbf{g}(t) = \begin{bmatrix} \mathbf{g}_1(t) \\ \mathbf{g}_2(t) \end{bmatrix}. \tag{.42}$$

With this partition, Equation (.2) becomes:

$$\frac{d\mathbf{x}_1(t)}{dt} = \mathbf{A}_{11}(t)\mathbf{x}_1(t) + \mathbf{A}_{12}(t)\mathbf{x}_2(t) + \mathbf{g}_1(t) \tag{.43}$$

$$\begin{aligned} \frac{d\mathbf{x}_2(t)}{dt} &= \mathbf{A}_{21}(t)\mathbf{x}_1(t) + \mathbf{A}_{22}(t)\mathbf{x}_2(t) + \mathbf{g}_2(t) \\ &= \mathbf{A}_{22}(t)\mathbf{x}_2(t) + \tilde{\mathbf{g}}(t), \end{aligned} \tag{.44}$$

where $\tilde{\mathbf{g}}(t) = \mathbf{A}_{21}(t)\mathbf{x}_1(t) + \mathbf{g}_2(t)$ is the nonhomogeneous part of Equation (.44), which has a fundamental matrix solution analogous to Equation (.38) as described by:

$$\mathbf{x}_2 = \int_{-\infty}^{t} \mathbf{K}_{22}(t,h)\tilde{\mathbf{g}}(h)dh, \tag{.45}$$

where $\mathbf{K}_{22}(t,h)$ is the fundamental matrix to $\mathbf{A}_{22}(t)$ of Equation (.44).

Thus, the unstructured model's equivalent of the structured model of Equation (.27) is now reduced to Equation (.44), whose more general form is:

$$\frac{d\mathbf{x}_1(t)}{dt} = \mathbf{f}_1(\mathbf{x}_1, \mathbf{x}_2, \mathbf{u}, t), \tag{.46}$$

where $\mathbf{x}_2$ is the time-lag integral defined by Equation (.45). If $\mathbf{x}_1(t)$ is composed of the biomass and limiting substrate concentrations as in our previous example, then $\mathbf{x}_2$ is simply the scalar observed specific growth rate, previously denoted y. Similarly, $\mathbf{u}$ is composed of control variables which, in our previous example, are the dilution rate, D, and the substrate concentration in the feed, s_f. $\mathbf{K}_{22}$ is the scalar time-lag kernel, k, and $\tilde{\mathbf{g}}$ is the scaler intrinsic specific growth rate, μ.

Note that Equation (.46) alone is the unstructured model; the addition of the information provided by the integral in Equation (.45) upgrades it to a structured model because these two combined equations are the *exact* equivalent of the original structured model described by Equation (.28). The time-lag kernel matrix $\mathbf{K}_{22}$ is the relationship that ties these two traditional modeling approaches. As can be seen from the preceeding equations, the time-lag kernel arises quite naturally as a consequence of reducing a larger set of dynamic equations of a structured model to a smaller set of dynamic equations of an unstructured model.

It is emphasized that the time-lag kernel is not simply an artificial mathematical concept; it is derived from a biological basis. Its presence can be explained by the fact that there exists a large collection of metabolic pathways and regulation steps. When a microorganism is subjected to a stimulus, it requires time for the cell to respond to the external stimuli as it adjusts its internal states one after another. For example, intermediate metabolites, precursors, enzymes, and various cofactors may be needed before the final product, which may be a specific enzyme, a chemical, or simply the cell biomass itself, can be assembled. Thus, the time-lag kernel compacts all our knowledge about the actual process of how a cell responds to the external stimuli into a simple functional form. It is the fundamental matrix to the missing dynamic equations. Conversely, a kernel has an equivalent representation in terms of structured dynamics. We see that a unique kernel can be constructed given the dynamics of the system, but the reconstruction of structure from a kernel function is not unique because more than one different process can be responsible for the same response and, thus, the same kernel function. In such a circumstance, the rule of modeling dictates that the simpler mechanism be chosen.

The kernel concept can be used to check the validity of the proposed mechanism in a structured model. For example, if the experimentally obtained kernel

function does not agree with that directly derived from the structured model, one can conclude that the original hypothesis is perhaps erroneous, and, as mentioned earlier, the shape of the kernel function can give one some insight as to the type of mechanism that may be responsible for the observed kernel. One may then revise his hypothesis and recheck to verify if the kernel function now conforms to the assumed mechanism. Alternatively, one may build a reasonably good structured model from some experimentally determined kernel functions. For example, if one were to find that the time-lag kernel could be approximated by a 0th-order exponential distribution function, then, based on the implied meaning of this kernel, one might plan further experiments aimed at identifying the rate limiting "critical enzyme." Thus, the kernel might be used to help suggest the type of experiment to be performed.

Examples of Structured Model Reduction:

The methodology on the reduction of a structured model to an unstructured model will be demonstrated by analyzing some typical structured models. Particular attention will be focused on the determination of whether a model indeed has structures and, if so, which state variables have structures. As mentioned previously, the appearance of a time-lag can be attributed to the process dynamics associated with the structure. The time-lag kernel associated with the neglected kinetic information when a structured model is reduced to an unstructured model will be derived theoretically.

Imanaka's Model of Enzyme Production: (Imanaka *et al., J. Ferment. Technol.*, **50**, 633, 1972.) One of the structured examples is Imanaka's model of enzyme (α-galactosidase) production developed for *Monascus* sp. The kinetic expressions are derived based on the operon theory of enzyme production. For a batch fermentor,

the model consists of the following set of eight dynamic equations:

Biomass: $$\frac{dX}{dt} = \mu X \tag{.47.1}$$

Glucose: $$\frac{dS_A}{dt} = -\frac{1}{Y_A}\mu_A X \tag{.47.2}$$

Galactose: $$\frac{dS_B}{dt} = -\frac{1}{Y_B}\mu_B X \tag{.47.3}$$

Intra. Galactose: $$\frac{ds_{Bi}}{dt} = U[\frac{G_B S_B}{K_{mB} + S_B} - s_{Bi}] - k_1 s_{Bi} - \mu s_{Bi} \tag{.47.4}$$

Repressor: $$\frac{dr}{dt} = k_2 - k_3 r - k_4 r \cdot s_{Bi} + k_5 \overline{rs_{Bi}} - \mu r \tag{.47.5}$$

Rep/Ind Complex: $$\frac{d\overline{rs_{Bi}}}{dt} = k_4 r \cdot s_{Bi} - k_5 \overline{rs_{Bi}} - \mu \overline{rs_{Bi}} \tag{.47.6}$$

mRNA: $$\frac{dm}{dt} = k_6(r_c - r) - k_7 m - \mu m \tag{.47.7}$$

Galactosidase: $$\frac{de}{dt} = k_8 m - \mu e \tag{.47.8}$$

In the above equations, the macroscopic variables X (biomass), S_A (glucose), and S_B (galactose) are expressed in concentration units of mg/(reactor volume); whereas, the intracellular components s_{Bi} (intracellular galactose), r (repressor), $\overline{rs_{Bi}}$ (repressor-inducer complex), m (messenger RNA), and e (α-galactosidase) are expressed in concentration units of mg/(g cell). Note that each of the dynamic equations for the intracellular components has a term that contains μ multiplied by the component itself. This term represents the dilution factor due to the expanding cell volume as the microorganism grows.

Similarly, for a continuous fermentor, the above set of equations become:

Biomass: $$\frac{dX}{dt} = \mu_X - DX \tag{.48.1}$$

Glucose: $$\frac{dS_A}{dt} = -\frac{1}{Y_A}\mu_A X + D(S_{Af} - S_A) \qquad (.48.2)$$

Galactose: $$\frac{dS_B}{dt} = -\frac{1}{Y_B}\mu_B X + D(S_{Bf} - S_B) \qquad (.48.3)$$

Intra. Galactose: $$\frac{dS_{Bi}}{dt} = U[\frac{G_B S_B X}{K_{mB} + S_B} - S_{Bi}] - k_1 S_{Bi} - DS_{Bi} \qquad (.48.4)$$

Repressor: $$\frac{dR}{dt} = k_2 X - k_3 R - k_4 \frac{R \cdot S_{Bi}}{X} + k_5 \overline{RS_{Bi}} - DR \qquad (.48.5)$$

Rep/Ind Complex: $$\frac{d\overline{RS_{Bi}}}{dt} = k_4 \frac{R \cdot S_{Bi}}{X} - k_5 \overline{RS_{Bi}} - D\overline{RS_{Bi}} \qquad (.48.6)$$

mRNA: $$\frac{dM}{dt} = k_6(R_c - R) - k_7 M - DM \qquad (.48.7)$$

Galactosidase: $$\frac{dE}{dt} = k_8 M - DE \qquad (.48.8)$$

As in the batch fermentor, X (biomass), S_A (glucose), and S_B (galactose) are expressed in concentration units of mg/(reactor volume). However, intracellular components S_{Bi} (intracellular galactose), R (repressor), $\overline{RS_{Bi}}$ (repressor-inducer complex), M (messenger RNA), and E (α-galactosidase) are expressed in concentration units of mg/(fermentor volume) in the above set of equations for a continuous fermentor. The symbols for the cellular volume-based variables are in lower case letters, and those for the fermentor volume-based variables are in upper case letters. This change of units is used to keep the two sets of equations in similar forms. These two sets of variables differ from each other by a factor of X:

$$S_{Bi} = X \cdot s_{Bi} \qquad (.49.a)$$

$$R = X \cdot r \qquad R_c = r_c \cdot r_c \qquad (.49.b)$$

$$\overline{RS_{Bi}} = X \cdot \overline{rs_{Bi}} \qquad (.49.c)$$

$$M = X \cdot m \tag{.49.d}$$

$$E = X \cdot e \tag{.49.e}$$

The first three of these equations describe the concentration variation of the major macroscopic components in the fermentor. These expressions are directly obtained from the well-known unstructured dynamic equations, with Monod-type of specific growth rate constitutive relationships.

$$\mu = \mu_A + \mu_B \tag{.50.a}$$

$$\mu_A = \frac{\mu_{mA} S_A}{K_{SA} + S_A + \frac{K_{SA}}{K_i} S_B} \tag{.50.b}$$

$$\mu_B = \begin{cases} \frac{\mu_{mB} S_B}{K_{SB} + S_B} & \text{for } S_A < S_{Ac} \\ 0 & \text{for } S_{Ac} \leq S_A \end{cases} \tag{.50.c}$$

Because these first three dynamic equations contain no state variables other than themselves, they are completely decoupled from the rest of the equations and can be solved independently of the enzyme production. Furthermore, because of this complete decoupling, there is no structure for the biomass, glucose, or galactose. Thus, there is no time-lag in the response of these variables.

However, the above statement does not hold true for the enzyme. As shown in Figure .1, there are five dynamic steps that separate the overall output (e) from the input (D, S_{Af}, and S_{Bf}). Thus, all the structure is contained in a sequence of events that finally lead to the enzyme production. The enzyme production requires the presence of mRNA (m), which is produced when the repressor level is below the critical level of r_c. Mathematically, this on/off event can be expressed as:

$$k_6 = \begin{cases} k_6 & \text{for } r < r_c \\ 0 & \text{for } r_c \leq r \end{cases} \tag{.51}$$

The repressor, in turn, is produced at a constant rate and is inactivated by combining with the inducer – the intracellular galactose (s_{Bi}). The transport of galactose

into the cell is effectively turned off when the fermentor glucose concentration exceeds a critical value of S_{Ac}. This statement is expressed mathematically as:

$$U = \begin{cases} U & \text{for } S_A < S_{Ac} \\ 0 & \text{for } S_{Ac} \leq S_A \end{cases} \tag{.52}$$

As the first example, the continuous fermentor with a step change in the dilution rate from D=1.40 hr^{-1} to D=1.42 hr^{-1} at t=0 hr is simulated with the above set of equations. The same set of model parameters claimed to be used by the original authors are employed to generate the concentration profiles. The values of the parameters used are reproduced below:

Experimental Model Values		
μ_{mA}	0.215	hr^{-1}
μ_{mA}	0.208	hr^{-1}
K_{SA}	0.154	g/l
K_{SB}	0.258	g/l
K_i	0.139	g/l
Y_A	0.530	g/g cell
Y_B	0.516	g/g cell

Undetermined Model Values		
k_1	40.	hr^{-1}
k_2	1.	mg/(g cell)-hr
k_3	1.	hr^{-1}
k_4	0.1	(g cell)/mg-hr
k_5	0.0001	hr^{-1}
k_6	1.	hr^{-1}
k_7	8.	hr^{-1}
k_8	4.	K unit/(mg mRNA)-hr
U	100.	hr^{-1}
G_2	3.5	mg/(g cell)-hr
K_{mB}	0.00000001	g/l

Critical Values		
S_{Ac}	0.225	g/l
r_c	0.803	mg/(g cell)

Operating Conditions		
D	$0.140 \rightarrow 0.142$	hr^{-1}
S_{fA}	20.	g/l
S_{fB}	5.	g/l

Initial Conditions		
X_0	13.	g/l
S_{A0}	0.223	g/l
S_{B0}	0.0501	g/l
s_{Bi0}	2.5	mg/(g cell)
r_0	0.718	mg/(g cell)
$\overline{rs_{Bi0}}$	1.28	mg/(g cell)
m_0	0.0104	mg/(g cell)
e_0	0.297	K units/(g cell)

The original authors' results are reproduced in Figure .2. The results of this author's simulation are shown in Figures .3 and .4. It should be noted that even after an extensive effort in experimenting with various sets of model parameters and the time of the dilution rate shift, the author was *unable* to obtain the type of behavior claimed by Imanaka *et al.* Because, as mentioned previously, the first three macroscopic variables are decoupled, these three dynamic equations can be analyzed independently of the rest of the equations. It is known that for a system described by Monod-style dynamics, a sudden increase in the glucose concentration shown in Figure .2 at t=7 hr is not possible unless some type of external disturbance is introduced at that instant. Alternatively, suppose the dilution rate were shifted at t=7 hr, there would also be sudden changes in the biomass and galactose concentrations at the same time, which are not present in the same figure.

The first step in expressing a structured model in a time-lag format is to identify the unstructured variables. In this example, the state vector for the unstructured

variables is:

$$\mathbf{x}_1(t) = \begin{bmatrix} X(t) \\ S_A(t) \\ S_B(t) \\ E(t) \end{bmatrix} \tag{.53}$$

The remaining intracellular variables are partitioned into $\mathbf{x}_2(t)$:

$$\mathbf{x}_2(t) = \begin{bmatrix} S_{Bi}(t) \\ R(t) \\ \overline{RS_{Bi}}(t) \\ M(t) \end{bmatrix} \tag{.54}$$

Thus, the equivalent unstructured model presented in the form of Equation (.46) is:

$$\underbrace{\begin{bmatrix} \frac{dX(t)}{dt} \\ \frac{dS_A(t)}{dt} \\ \frac{dS_B(t)}{dt} \\ \frac{dE(t)}{dt} \end{bmatrix}}_{\frac{d\mathbf{x}_1(t)}{dt}} = \underbrace{\begin{bmatrix} \mu_X - DX \\ -\frac{1}{Y_A}\mu_A X + D(S_{Af} - S_A) \\ -\frac{1}{Y_B}\mu_B X + D(S_{Bf} - S_B) \\ k_8 M - DE \end{bmatrix}}_{\mathbf{f}_1(\mathbf{x}_1, \mathbf{x}_2, \mathbf{u}, t)} \tag{.55}$$

The above equation indicates that there is a single time-lag variable M in the dynamics of enzyme formation. The time-lag kernel differential equation can be obtained for this multidimensional system from the dynamics of $\mathbf{x}_2(t)$. Following

Equation (.44), the linearized dynamics of $\mathbf{x}_2(t)$ is expressed as:

$$\underbrace{\begin{bmatrix} \frac{dS_{Bi}(t)}{dt} \\ \frac{dR(t)}{dt} \\ \frac{d\overline{RS_{Bi}}}{dt} \\ \frac{dM(t)}{dt} \end{bmatrix}}_{\frac{d\mathbf{x}_2(t)}{dt}} =$$

$$\underbrace{\begin{bmatrix} -U-k_1-D & 0 & 0 & 0 \\ -\frac{k_4R_0}{X_0} & -\frac{k_4S_{Bi0}}{X_0}-k_3-D & k_5 & 0 \\ \frac{k_4R_0}{X_0} & \frac{k_4S_{Bi0}}{X_0} & -k_5-D & 0 \\ 0 & -k_6 & 0 & -k_7-D \end{bmatrix}}_{\mathbf{A}_{22}(t)} \underbrace{\begin{bmatrix} S_{Bi}(t) \\ R(t) \\ \overline{RS_{Bi}}(t) \\ M(t) \end{bmatrix}}_{\mathbf{x}_2(t)}$$

$$+ \underbrace{\begin{bmatrix} U\frac{G_BS_B(t)X(t)}{K_{mB}+S_B(t)} \\ \left[k_2+\frac{k_4R_0S_{Bi0}}{X_0^2}\right]X(t) \\ -\frac{k_4R_0S_{Bi0}}{X_0^2}X(t) \\ k_6r_cX(t) \end{bmatrix}}_{\tilde{\mathbf{g}}(t)} \tag{.56}$$

The solution of the above set of dynamic equations is expressed in the time-lag kernel matrix form of Equation (.45) as:

$$\begin{aligned} \mathbf{x}_2(t) &= \int_{-\infty}^{t} \underbrace{e^{\mathbf{A}_{22}(t-h)}}_{\mathbf{K}_{22}(t-h)} \tilde{\mathbf{g}}(h)dh \\ &= \int_{-\infty}^{t} \mathbf{K}_{22}(t-h)\tilde{\mathbf{g}}(h)dh. \end{aligned} \tag{.57}$$

Thus, the time-lag variable M(t) in Equation (.55) can be expressed in an equivalent kernel integral format as:

$$\begin{aligned} M(t) = \int_{-\infty}^{t} \Bigg[& k_{41}(t-h)U\left[\frac{G_BS_B(h)}{K_{mB}+S_B(h)}\right] + k_{42}(t-h)\left[k_2+\frac{k_4R_0S_{Bi0}}{X_0^2}\right] \\ & \cdot -k_{43}(t-h)\frac{k_4R_0S_{Bi0}}{X_0^2} + k_{44}(t-h)k_6r_c\Bigg]X(h)dh, \end{aligned} \tag{.58}$$

where $k_{ij}(t)$ is the ijth element of the matrix exponential $e^{\mathbf{A}_{22}t}$.

The above equation can be simplified for the dilution rate shift-up example. Because of the large value of U, the dynamics of s_{Bi} is fast, and s_{Bi} is zero for the most part. Thus, its dynamics can be ignored to reduce the dimension of the system by 1 in order to facilitate greatly the mathematical analysis. With $s_{Bi} = 0$, Equation (.56) becomes:

$$\underbrace{\begin{bmatrix} \frac{dR(t)}{dt} \\ \frac{d\overline{RS_{Bi}}}{dt} \\ \frac{dM(t)}{dt} \end{bmatrix}}_{\frac{d\mathbf{x}_2(t)}{dt}} = \underbrace{\begin{bmatrix} -k_3 - D & k_5 & 0 \\ 0 & -k_5 - D & 0 \\ -k_6 & 0 & -k_7 - D \end{bmatrix}}_{\mathbf{A}_{22}(t)} \underbrace{\begin{bmatrix} R(t) \\ \overline{RS_{Bi}}(t) \\ M(t) \end{bmatrix}}_{\mathbf{x}_2(t)} + \underbrace{\begin{bmatrix} k_2 X(t) \\ 0 \\ k_6 r_c X(t) \end{bmatrix}}_{\tilde{\mathbf{g}}(t)} \tag{.59}$$

Note that linearization is not necessary with $s_{Bi} = 0$. At D=0.142 hr^{-1}, substituting the numerical values for the model parameters into $\mathbf{A}_{22}$ gives:

$$\mathbf{A}_{22} = \begin{bmatrix} -1.142 & 0.0001 & 0 \\ 0 & -0.1421 & 0 \\ -1 & 0 & -0.8142 \end{bmatrix} \tag{.60}$$

$$\begin{aligned} 0 = \det|\mathbf{A}_{22} - \lambda\mathbf{I}| &= \begin{vmatrix} -1.142 - \lambda & 0.0001 & 0 \\ 0 & -0.1421 - \lambda & 0 \\ -1 & 0 & -8.142 - \lambda \end{vmatrix} \\ &= (-1.142 - \lambda)(-0.1421 - \lambda)(-8.142 - \lambda) \end{aligned} \tag{.61}$$

$$\Longrightarrow \qquad \lambda_1 = -1.142 \qquad \lambda_2 = -0.1421 \qquad \lambda_3 = -8.142 \tag{.62a}$$

$$\Longrightarrow \qquad \mathbf{T} = \begin{bmatrix} -7 & -7.9999 & 0 \\ 0 & -79991.0001 & 0 \\ 1 & 1 & 1 \end{bmatrix} \qquad \mathbf{T}^{-1} = \begin{bmatrix} -0.1429 & 1.43 \times 10^{-5} & 0 \\ 0 & -1.25 \times 10^{-5} & 0 \\ 0.1429 & -1.79 \times 10^{-6} & 1 \end{bmatrix} \tag{.62b}$$

$$\begin{aligned} \mathbf{K}(t) = e^{\mathbf{A}_{22}t} &= \begin{bmatrix} k_{11}(t) & k_{12}(t) & k_{13}(t) \\ k_{21}(t) & k_{22}(t) & k_{23}(t) \\ k_{31}(t) & k_{32}(t) & k_{33}(t) \end{bmatrix} \\ &= \underbrace{\begin{bmatrix} -7 & -7.9999 & 0 \\ 0 & -79991.0001 & 0 \\ 1 & 1 & 1 \end{bmatrix}}_{\mathbf{T}} \underbrace{\begin{bmatrix} e^{\lambda_1 t} & 0 & 0 \\ 0 & e^{\lambda_2 t} & 0 \\ 0 & 0 & e^{\lambda_3 t} \end{bmatrix}}_{e^{\mathbf{J}t}} \underbrace{\begin{bmatrix} -0.1429 & 1.43 \times 10^{-5} & 0 \\ 0 & -1.25 \times 10^{-5} & 0 \\ 0.1429 & -1.79 \times 10^{-6} & 1 \end{bmatrix}}_{\mathbf{T}^{-1}} \\ &= \begin{bmatrix} e^{\lambda_1 t} & \approx 0 & 0 \\ 0 & e^{\lambda_2 t} & 0 \\ 0.1429(e^{\lambda_3 t} - e^{\lambda_1 t}) & \approx 0 & e^{\lambda_3 t} \end{bmatrix} \end{aligned} \tag{.63c}$$

With the given initial conditions, Equation (.57) is now reduced to:

$$\underbrace{\begin{bmatrix} R(t) \\ \overline{RS_{Bi}}(t) \\ M(t) \end{bmatrix}}_{\mathbf{x}_2(t))} = \underbrace{\begin{bmatrix} k_{11}(t) & k_{12}(t) & k_{13}(t) \\ k_{21}(t) & k_{22}(t) & k_{23}(t) \\ k_{31}(t) & k_{32}(t) & k_{33}(t) \end{bmatrix}}_{\mathbf{K}_{22}(t)} \underbrace{\begin{bmatrix} R(0) \\ \overline{RS_{Bi}}(0) \\ M(0) \end{bmatrix}}_{\mathbf{x}_2(0)}$$
$$+ \int_0^t \underbrace{\begin{bmatrix} k_{11}(t-h) & k_{12}(t-h) & k_{13}(t-h) \\ k_{21}(t-h) & k_{22}(t-h) & k_{23}(t-h) \\ k_{31}(t-h) & k_{32}(t-h) & k_{33}(t-h) \end{bmatrix}}_{\mathbf{K}_{22}(t-h)} \underbrace{\begin{bmatrix} k_2 X(h) \\ 0 \\ k_6 r_c X(h) \end{bmatrix}}_{\tilde{\mathbf{g}}(h)} dh \tag{.63}$$

Finally, the time-lag variable $M(t)$ is described by the following kernel integral:

$$\begin{aligned} M(t) &= \int_{-\infty}^{t} \underbrace{\left\{0.1429\left(e^{\lambda_3(t-h)} - e^{\lambda_1(t-h)}\right) + 0.803e^{\lambda_3(t-h)}\right\}}_{k(t-h)} X(h)dh \\ &= 0.1429\left(e^{\lambda_3 t} - e^{\lambda_1 t}\right)R(0) + e^{\lambda_3 t}M(0) \\ &\quad + \int_0^t \left\{0.1429\left(e^{\lambda_3(t-h)} - e^{\lambda_1(t-h)}\right) + 0.803e^{\lambda_3(t-h)}\right\} X(h)dh. \end{aligned} \tag{.64}$$

Note that for $k_6 = 0$, the above equation is reduced to:

$$M(t) = e^{\lambda_3 t}M(0), \tag{.65}$$

and there is no time-lag in the response of the enzyme because all the terms in the time-lag integral are practically equal to zero.

In Figure .5, the enzyme profile calculated with the time-lag approach, with a kernel described by Equation (.64), is contrasted with that calculated by integrating the full set of eight dynamic equations. The kernel is turned on when $S_A < S_{Ac}$. Note that this critical point can be determined with the unstructured variables, and no knowledge of the process structure of enzyme induction and repression is used in the time-lag calculation. It is apparent that there is no visible difference between the two curves. Also shown in the same figure is the enzyme level as a function of time, calculated with Equation (.65) for the entire duration. Since the dynamic equations for biomass, glucose, and galactose concentrations are unstructured, there

is absolutely no difference in calculated results of these variables, whether a full set of equations is used or not.

The next example is the simulation of enzyme production in a batch mode. For reference purposes, Imanaka *et al.*'s experimental results and model prediction are reproduced in Figure .6. As in the continuous mode of operation, this author was unable to reproduce the same curves with the model and parameters provided by Imanaka *et al.*, although the overall features of the obtainable batch fermentation are comparable. The following is a list of the model parameters that were used that differ from the ones used in the previous example of continuous fermentation, due to the different operating conditions (temperature, nutrient composition, etc.)

Experimental Model Values		
μ_{mA}	0.190	hr^{-1}
μ_{mB}	0.162	hr^{-1}
K_{SA}	0.145	g/l
K_{SB}	0.307	g/l
Y_A	0.377	g/g cell
Y_B	0.361	g/g cell

Undetermined Model Values		
k_8	6.67	K unit/(mg mRNA)-hr

Initial Conditions		
X_0	0.5	g/l
S_{A0}	10.	g/l
S_{B0}	3.	g/l
s_{Bi0}	0.	mg/(g cell)
r_0	0.91	mg/(g cell)
$\overline{rs_{Bi0}}$	0.	mg/(g cell)
m_0	0.	mg/(g cell)
e_0	0.	K units/(g cell)

The simulated results calculated with a full set of eight dynamic equations are plotted in Figures .7 and .8. The enzyme concentration for the time-lag approach, shown in Figure .9, is calculated based on the following dynamic equation:

$$\frac{de(t)}{dt} = k_8 m(t) - \mu e(t), \tag{.66}$$

where the time-lag variable $m(t)$ is activated at the time when S_A becomes smaller than the critical glucose concentration of S_{Ac}. This critical time, denoted as t_c, can be determined from the macroscopic variables without the knowledge of the structure of enzyme production. The slight deviation is due to the fact that the enzyme profile determined by the full set of dynamic equations is based on the internal on/off mechanism of mRNA production, which depends on the value of $(r_c - r)$. This value is not available to an unstructured model that does not consider the internal mechanisms, and the closest on/off switch available to an unstructured model is the crossing of S_{Ac} by S_A. In view of the fact that only macroscopic variables are used to generate the concentration profiles, the agreement is quite good.

The equivalent time-lag kernel for the batch case can be derived from Equations (.47.4)–(.47.7). As before, instead of manipulating the entire set of equations simultaneously, it is beneficial to make some simplifications. Because U and k_1 are large, one can apply the quasi-steady state assumption to s_{Bi}. Furthermore, because K_{mB} is extremely small, one can assume that $\frac{G_B S_B}{K_{mB}+S_B} = G_B$ for $S_B > K_{mB}$. This leads to:

$$0 = \frac{ds_{Bi}}{dt} = U(G_B - s_{Bi}) - k_1 s_{Bi} - \mu s_{Bi} \tag{.67a}$$

$$s_{Bi} \approx \frac{UG_B}{U + k_1 + \mu} \approx \frac{UG_B}{U + k_1} = 2.5 \quad \text{for} \quad \begin{matrix} S_A < S_{Ac} \\ \& \; S_B > K_{mB} \end{matrix} \tag{.67b}$$

With this simplification, a matrix equation similar to Equation (.59) can be obtained:

$$\underbrace{\begin{bmatrix} \frac{dr(t)}{dt} \\ \frac{d\overline{rs}_{Bi}}{dt} \\ \frac{dm(t)}{dt} \end{bmatrix}}_{\frac{d\mathbf{x}_2(t)}{dt}} = \underbrace{\begin{bmatrix} -k_4 s_{Bi} - k_3 - \mu & k_5 & 0 \\ k_4 s_{Bi} & -k_5 - \mu & 0 \\ -k_6 & 0 & -k_7 - \mu \end{bmatrix}}_{\mathbf{A}_{22}(t)} \underbrace{\begin{bmatrix} r(t) \\ \overline{rs}_{Bi}(t) \\ m(t) \end{bmatrix}}_{\mathbf{x}_2(t)} + \underbrace{\begin{bmatrix} k_2 \\ 0 \\ k_6 r_c \end{bmatrix}}_{\tilde{\mathbf{g}}(t)} \tag{.68}$$

The dynamic matrix, after substituting model parameters, is:

$$\mathbf{A}_{22} = \begin{bmatrix} -1.25 - \mu & 0.0001 & 0 \\ 0.25 & 0.0001 - \mu & 0 \\ -1 & 0 & -8 - \mu \end{bmatrix} \approx \begin{bmatrix} -1.25 - \mu & 0 & 0 \\ 0.25 & -\mu & 0 \\ -1 & 0 & -8 - \mu \end{bmatrix} \tag{.69}$$

$$\begin{aligned} 0 = \det|\mathbf{A}_{22} - \lambda \mathbf{I}| &= \begin{vmatrix} -1.25 - \mu - \lambda & 0 & 0 \\ 0.25 & -\mu - \lambda & 0 \\ -1 & 0 & -8 - \mu - \lambda \end{vmatrix} \\ &= (-1.25 - \mu - \lambda)(-\mu - \lambda)(-8 - \mu - \lambda) \end{aligned} \tag{.70}$$

$$\Longrightarrow \qquad \lambda_1 = -1.25 - \mu \qquad \lambda_2 = -\mu \qquad \lambda_3 = -8 - \mu \tag{.71a}$$

$$\Longrightarrow \quad \mathbf{T} = \begin{bmatrix} -6.75 & 0 & 0 \\ 1.35 & 1 & 0 \\ 1 & 0 & 1 \end{bmatrix} \qquad \mathbf{T}^{-1} = \begin{bmatrix} -\frac{1}{6.75} & 0 & 0 \\ 0.2 & 1 & 0 \\ \frac{1}{6.75} & 0 & 1 \end{bmatrix} \tag{.71b}$$

$$\mathbf{K}(t) = e^{\mathbf{A}_{22}t} = \underbrace{\begin{bmatrix} -6.75 & 0 & 0 \\ 1.35 & 1 & 0 \\ 1 & 0 & 1 \end{bmatrix}}_{\mathbf{T}} \underbrace{\begin{bmatrix} e^{\lambda_1 t} & 0 & 0 \\ 0 & e^{\lambda_2 t} & 0 \\ 0 & 0 & e^{\lambda_3 t} \end{bmatrix}}_{e^{\mathbf{J}t}} \underbrace{\begin{bmatrix} -\frac{1}{6.75} & 0 & 0 \\ 0.2 & 1 & 0 \\ \frac{1}{6.75} & 0 & 1 \end{bmatrix}}_{\mathbf{T}^{-1}} \tag{.71c}$$

$$= \begin{bmatrix} e^{\lambda_1 t} & \approx 0 & 0 \\ 0.2(e^{\lambda_2 t} - e^{\lambda_1 t}) & e^{\lambda_2 t} & 0 \\ \frac{1}{6.75}(e^{\lambda_3 t} - e^{\lambda_1 t}) & \approx 0 & e^{\lambda_3 t} \end{bmatrix}$$

Finally, the time-lag variable for the batch fermentation is:

$$m(t) = \begin{cases} 0 & \text{for } t \le t_c \\ m_{t_c} + \int_{t_c}^{t} k(t-h)X(h)dh & \text{for } t_c < t \end{cases}, \tag{.72}$$

where the kernel $k(t)$ is described by:

$$\begin{aligned} k(t) &= \frac{1}{6.75}\left(e^{\lambda_3 t} - e^{\lambda_1 t}\right) + 0.803e^{\lambda_3 t} \\ &= 0.9511e^{\lambda_3 t} - 0.1481e^{\lambda_1 t} \end{aligned} \tag{.73a}$$

and the pre-integral factor m_{t_c} used to absorb all the information between $t = -\infty$ and $t = t_c$ is:

$$\begin{aligned} m_{t_c} &= \frac{1}{6.75}\left(e^{\lambda_3 t} - e^{\lambda_1 t}\right) r(t_c) + e^{\lambda_3 t}\overset{0}{m}(t_c) \\ &\approx \frac{1}{6.75}\left(e^{\lambda_3 t} - e^{\lambda_1 t}\right) r_c. \end{aligned} \tag{.73b}$$

DISCUSSION

In summary, one of the attractions of using a complicated structured model is that is can be used to predict the bioreactor behavior under various operating conditions, provided that the kinetic steps are properly identified and all the model parameters are correctly assigned. Through literature example in this paper, it is shown that some of the dynamic steps in a structured model can be eliminated without seriously affecting the predicted output. Furthermore, a structured model can be reduced to an unstructured model with the difference being absorbed by the time-lag kernel. In model translation/reduction, it is often convenient to quasi-linearize a set of nonlinear differential equations. The next logical step is to analyze the eigenvalue and eigenvector of the linearized dynamic matrix $\mathbf{A}(t)$. Such an

analysis can yield useful information on the relative time scales of various processes. After grouping variables properly according to the process time constants, one can simplify and reduce the dimension of the system by retaining only the first few most important modes. Eliminating the remaining nonsignificant modes, like pruning a tree, helps to clarify the main feature of the model.

Parametric vs. Non-Parametric Modeling Approaches:

In conjunction with the discussion on the connection between a structured model and an unstructured model, it should be noted that our time-lag kernel modeling approach can also be viewed as a combination of other two opposing modeling approaches. One such example is the classification of models based on the presence or absence of differential and algebraic equations in the description of the process dynamics.

One of the methods of model classification is based on the representation of one's knowledge. A model can be classified as *parametric* if a *parameter space* is used to describe the process dynamics. In this approach, one's knowledge about the system under consideration is translated into a set of mathematical equations in terms of differential dynamic relationships supplemented, if necessary, by algebraic constitutive relationships. The output of the system is completely determined once one is supplied with the model parameters, initial conditions, and forcing functions. Properly viewed, both the initial conditions and forcing functions may also be considered as additional parameters. The dimensionality of the description in a parametric model is finite.

On the other hand, a *non-parametric model* of a black box type is also frequently used to describe the system dynamics when one's knowledge about the system is poor or when the system is complicated and its description cannot be easily reduced to mathematical equations. The characterization of the system is

carried out in a *function space* without resorting to the use of differential equations. For example, one may choose to use Fourier series expansions, spectral densities, autocovariance and cross-covariance matrices, time series, or impulse response and, of course, time-lag kernel functions. One or more of these relationships may be used to transform the forcing input to the system output without assuming the underlying structure of the process. These models are in principle infinitely dimensioned.

The advantage of a parametric model, being finite dimensioned, is that the system can be described concisely with a finite number of parameters. However, there is a price to be paid for this conciseness in terms of large prediction errors if the system orders or model parameters are not correctly chosen. If the system is complicated or if one cannot make valid assumptions regarding the physical process structure with a certain degree of confidence, then a non-parametric model may be advantageous. Because such a non-parametric model may be infinitely dimensioned, it has the capability of yielding a system output that matches exactly with the observation.

The proposed kernel modeling approach is a hybrid of the parametric and non-parametric approaches. See Figure .10. For example, state dynamic equations are written explicitly for those variables whose dynamics are well known. There is absolutely no doubt that the state equations for the biomass and substrate concentrations in a chemostat are valid if cell growth is regulated by a limiting substrate. These dynamic equations for macroscopic variables are derived based strictly on material balance concepts; all other effects can be treated as variations in the specific growth rate and/or the yield coefficient. Thus, one can justifiably use a parametric approach to model the macroscopic observations.

On the other hand, one often does not know enough about the dependence of the specific growth rate on other variables. Under these circumstances, it is not

practical to derive the dynamic equations for the specific growth rate. In such an attempt, sound judgment must be made as to what to assume and what to ignore, and these assumptions must be verified. In specifying the dynamic equations, the model orders must be known, and functional forms must be supplied. One often uses saturation functions of the Michaelis-Menten type whenever rate expressions are called for, but how often, if ever, are these expressions experimentally justified? Bimolecular elementary reaction rate expressions are often used also, but few studies have actually been conducted with the same degree of rigor that is demanded in the traditional proposal of a chemical reaction mechanism. Model discrimination is seldom performed in biochemical engineering. The moment one *single* such expression is inserted into a dynamic equation without independent verifications, the model complexity becomes superficial. It contains essentially a black box at this level. More complexity beyond this point is inconsequential because patterns contained inside a black box cannot be seen.

A complex parametric description usually contains numerous model parameters whose values must somehow be evaluated, in addition to the model's sensitivities to variations in the parameters. As pointed out previously, the predicted system behavior can be drastically different if the system order, functional form, or model parameters are not chosen correctly. It has the inherent danger that the entire model can crumble if there exists a weak link in the model such as an incorrect assumption.

Thus, for the part of the process whose dynamics are well-known, one can employ the parametric modeling approach. Whereas, for the part that either is too complicated to be expressed mathematically with confidence or calls for excess investment of resources, one can resort to a non-parametric description. This combined approach is especially suited for a system where the level of understanding is

not uniform across the process substructure. And many examples exist in biochemical engineering where the understanding of the process is quite nonuniform. It is not unusual that one can write the differential equations for macroscopic or lumped variables that can be easily quantified (unstructured modeling), but the dynamics for the intracellular components are often vague. One sacrifices knowledge of the process if a purely non-parametric approach is to be taken. On the other hand, one often needs to surpass his means if a purely parametric approach is taken. By using the combined approach, one can optimize effort by fully utilizing the current knowledge, without the danger of overreaching.

One example of such combined modeling approaches is the time-lag chemostat system demonstrated throughout this thesis; it uses differential equations for the biomass and substrate concentrations but gracefully switches to a time-lag kernel relationship to transform the input disturbance in the limiting substrate concentration to the observed specific growth rate. It should be emphasized that the chemostat example is used mainly to illustrate the time-lag approach. By no means does this simple example insist on the use of a time-lag kernel at level of the specific growth rate. If one is quite certain on the dynamics of certain intracellular components, then dynamic equations can be written for these components, and time-lag kernels can be employed for more intricate lower level sub-processes. It is only natural that the transition between a parametric approach and a non-parametric approach should be based on one's judgement as to which level his understanding of the process becomes vague. One should identify the level at which further structural refinement becomes superfluous due to the lack of actual knowledge. There is no need for a time-lag kernel if one's application does not demand accuracy beyond this point. Otherwise, the use of a time-lag kernel is recommended to compensate for the lack of detailed knowledge.

Since a model is to be judged based on its intended purpose, in many applications a time-lag kernel approach is a viable, attractive alternative to either an oversimplified unstructured model (abridged parametric model) that does not perform adequately, an overly complex structured model (fully developed parametric model) whose detailed description is unnecessary, or a purely black box approach (non-parametric model) that has little appeal due to the total lack of process structures.

BLOCK DIAGRAM OF IMANAKA'S MODEL

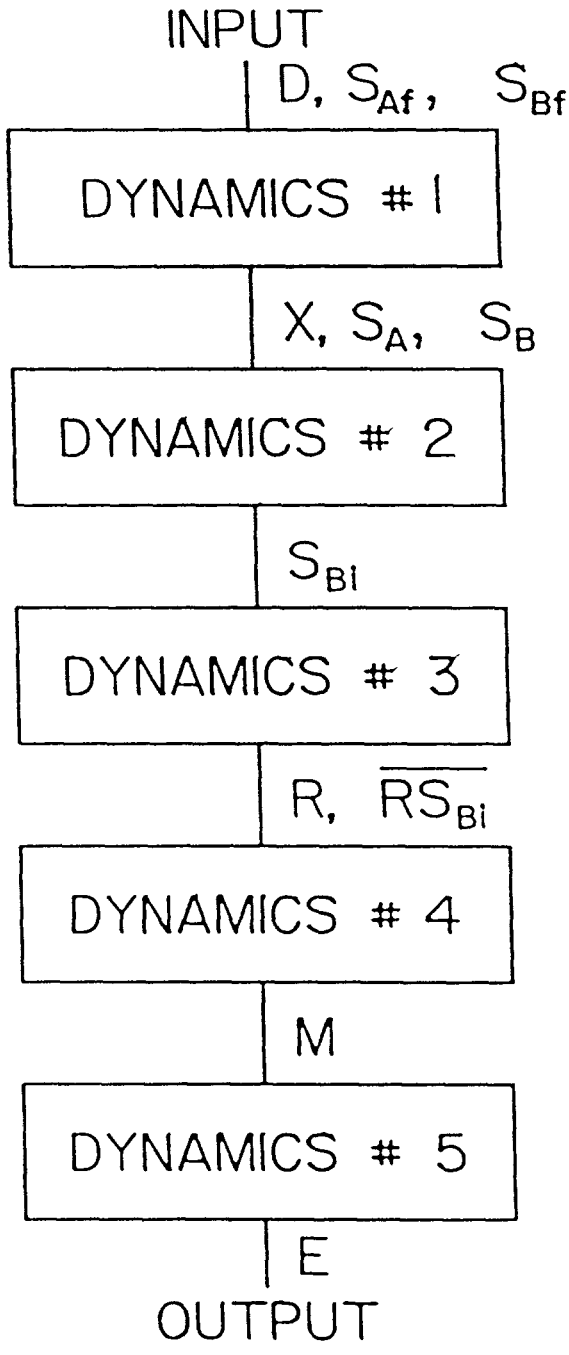

Figure 1. Steps leading to the formation of galactosidase.

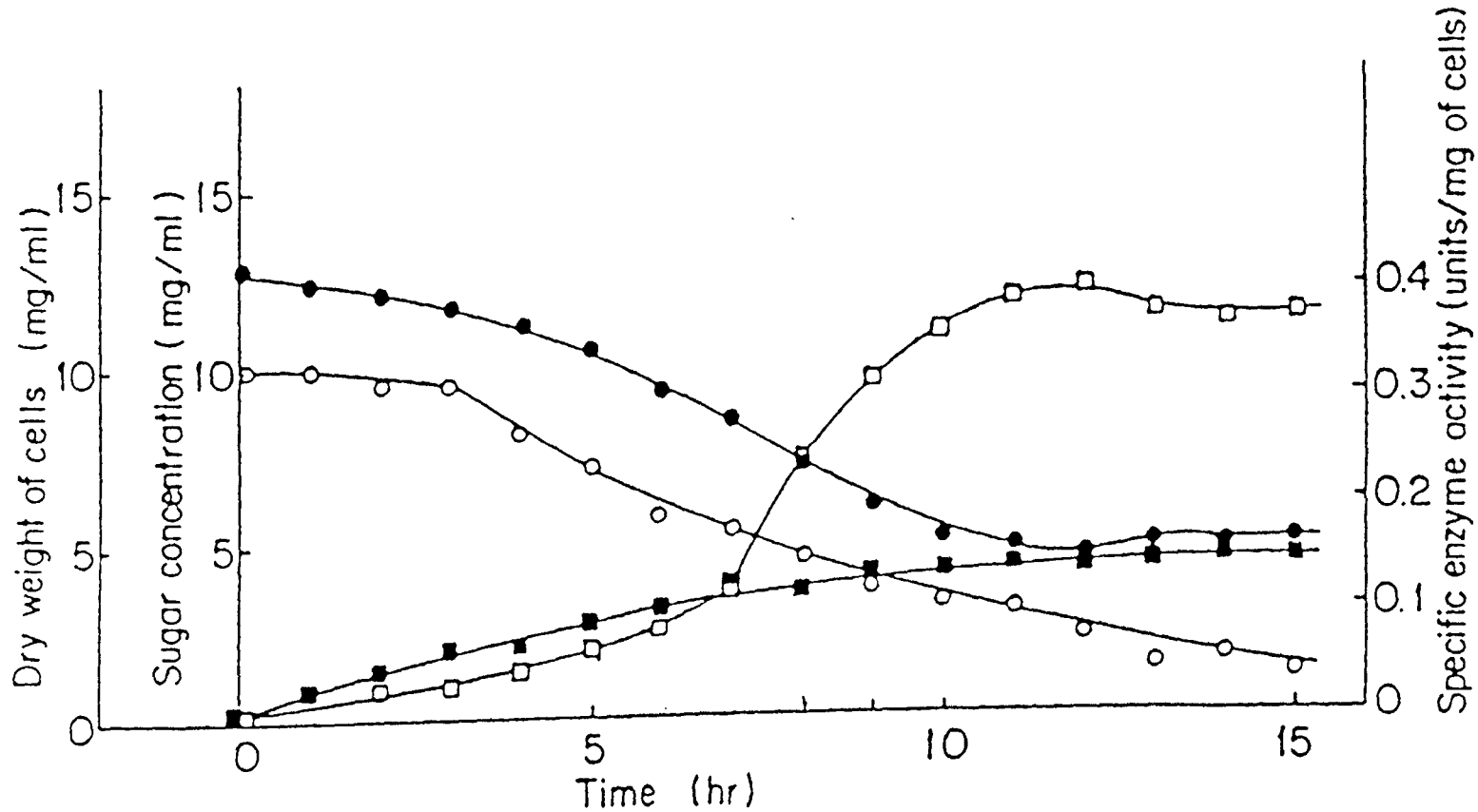

Figure 2. Transient behavior in a single-stage continuous culture. Glucose (2%) and galactose (0.5%) were used as carbon sources. The dilution rate was changed from 0.140 to 0.142 hr^{-1}. Reproduced from Imanaka *et al.* (1973).

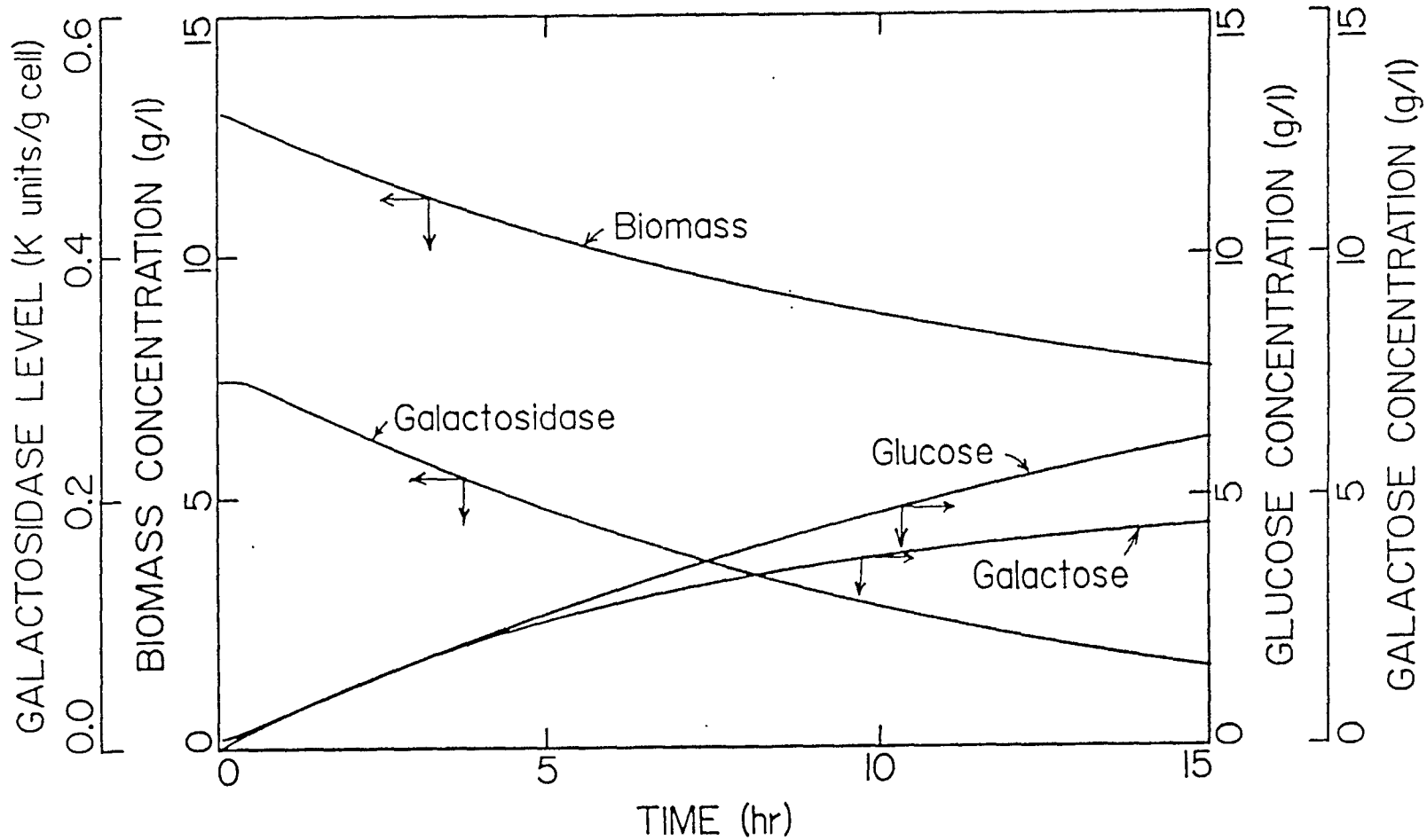

Figure 3. Time profile of macroscopic state variables (biomass, glucose, galactose, and enzyme) after a shift up in the dilution rate from 1.40 hr^{-1} to 1.42 hr^{-1} at t=0 hr. See text for the values of model parameters and initial conditions.

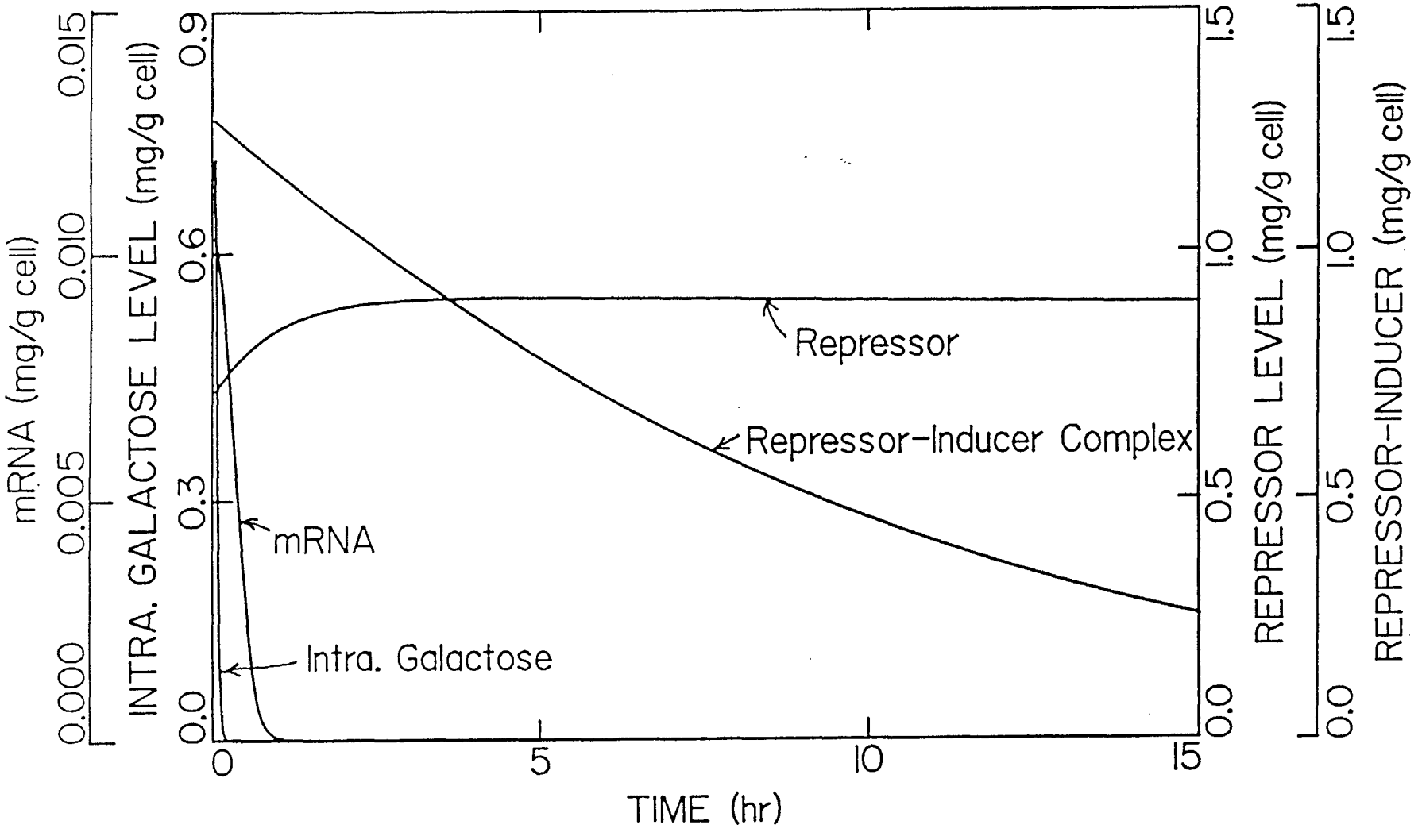

Figure 4. Time profile of intracellular state variables (intracellular galactose, repressor, repressor-inducer complex, and mRNA) after a shift up in the dilution rate from 1.40 hr^{-1} to 1.42 hr^{-1} at t=0 hr. See text for the values of model parameters and initial conditions.

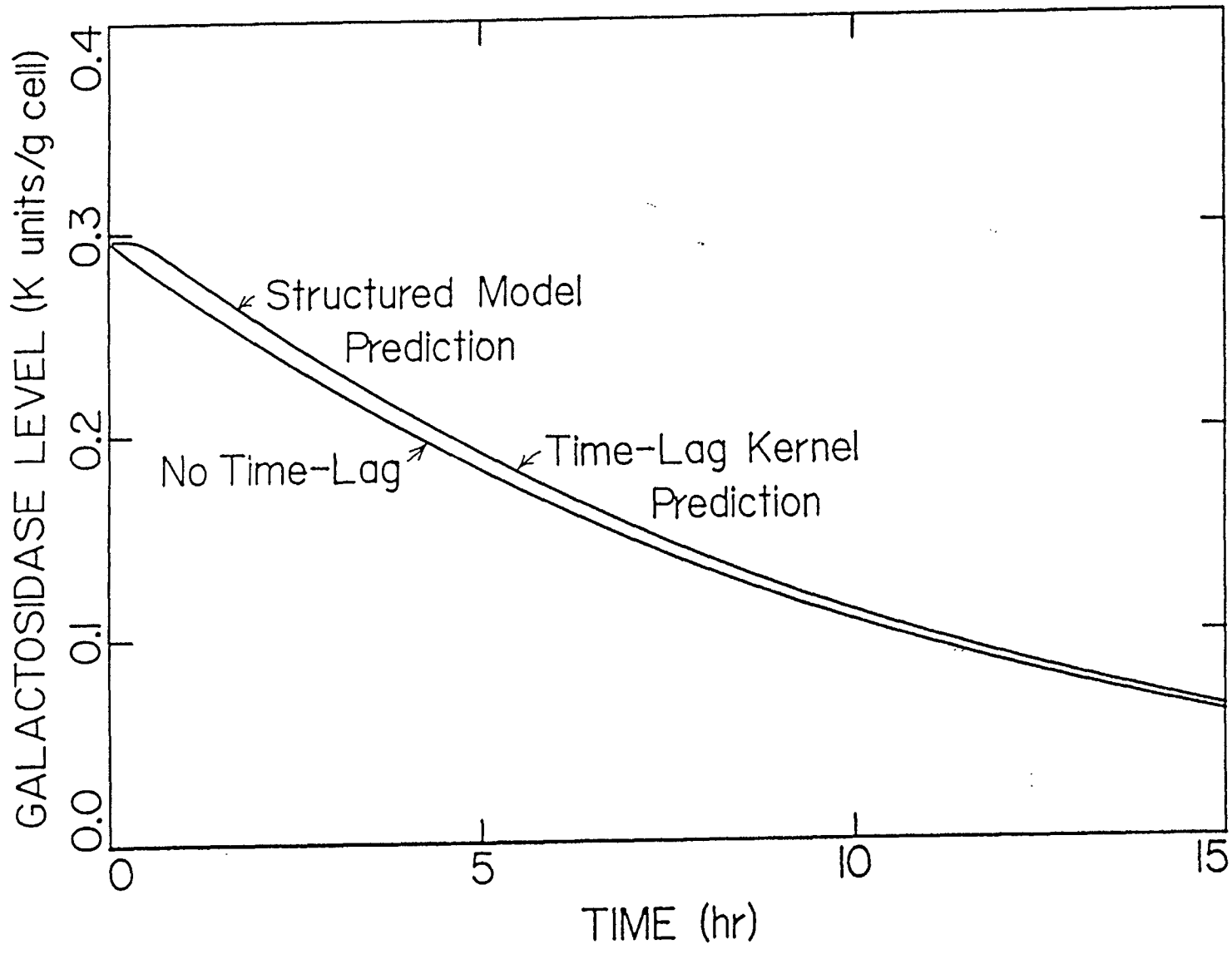

Figure 5. Comparison of the enzyme profiles calculated with Imanaka's structured model of enzyme production and the time-lag kernel approach after a shift up in the dilution rate from 1.40 hr^{-1} to 1.42 hr^{-1} at t=0 hr.

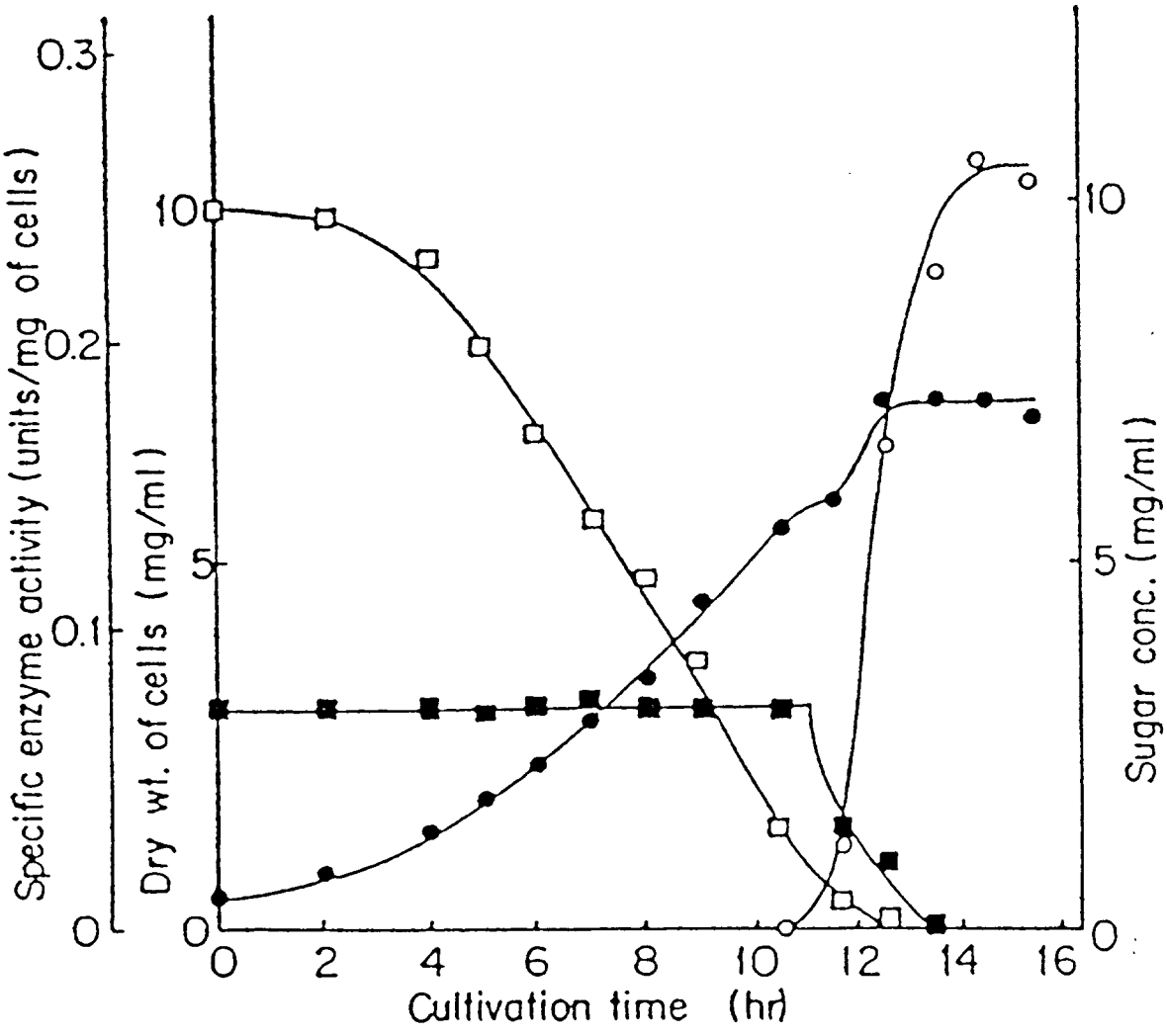

Figure 6. Time course of cell growth and α-galactosidase production in a mixture of glucose (1%) and galactose (0.3%). Reproduced from Imanaka *et al.* (1973).

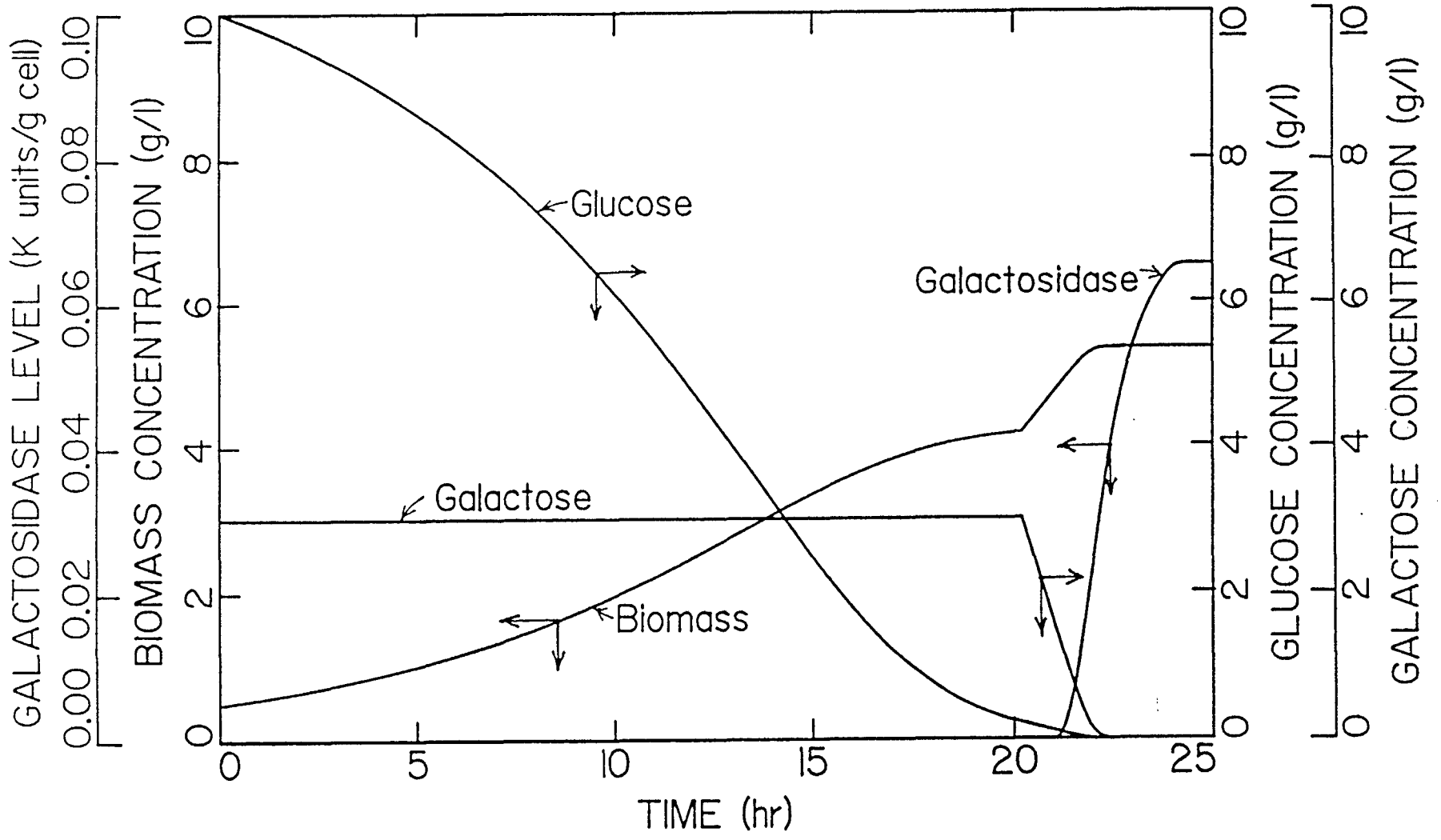

Figure 7. Time profile of macroscopic state variables (biomass, glucose, galactose, and enzyme) in the batch production of α-galactosidase. See text for the values of model parameters and initial conditions.

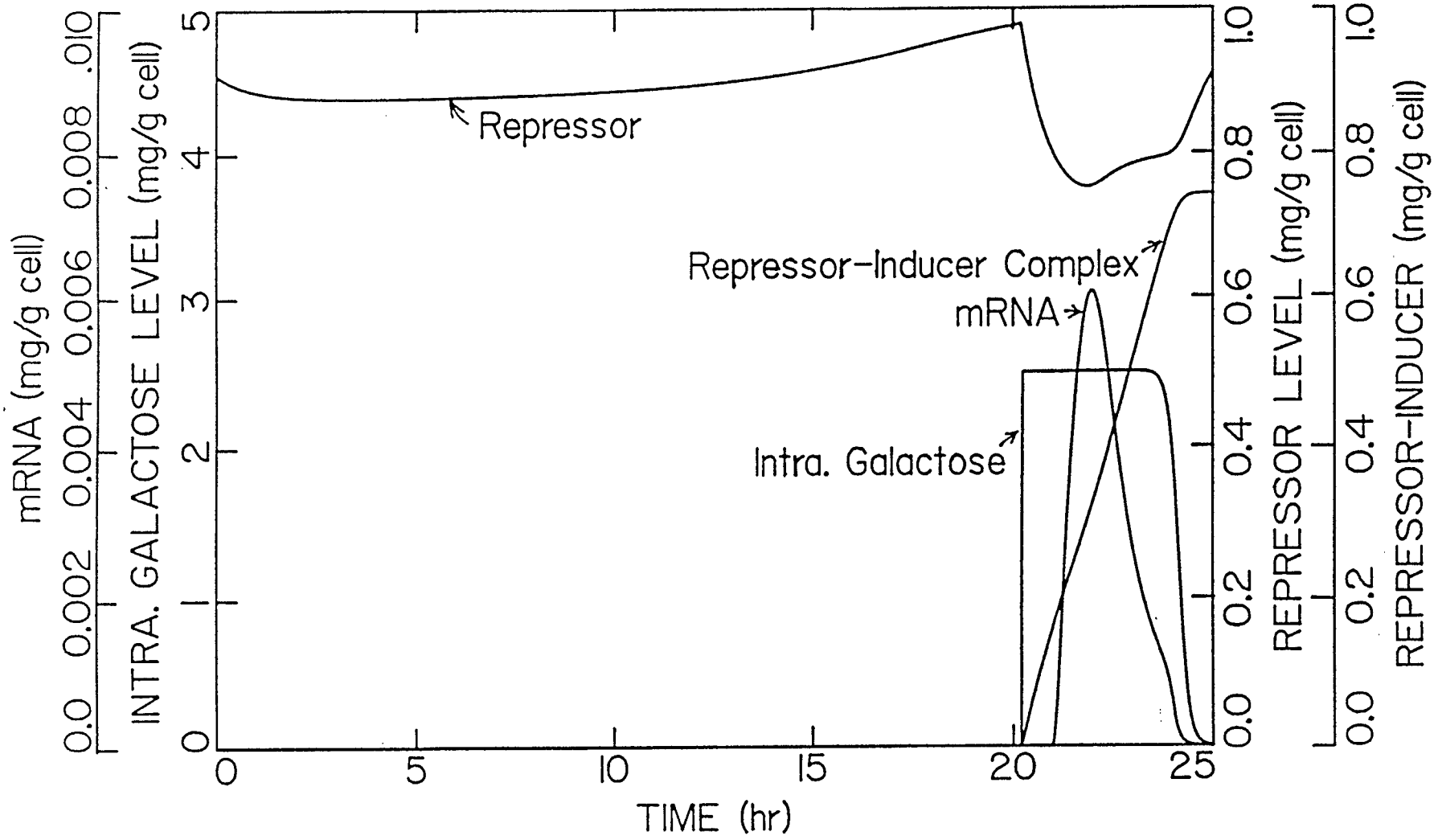

Figure 8. Time profile of intracellular state variables (intracellular galactose, repressor, repressor-inducer complex, and mRNA) in the batch production of α-galactosidase. See text for the values of model parameters and initial conditions.

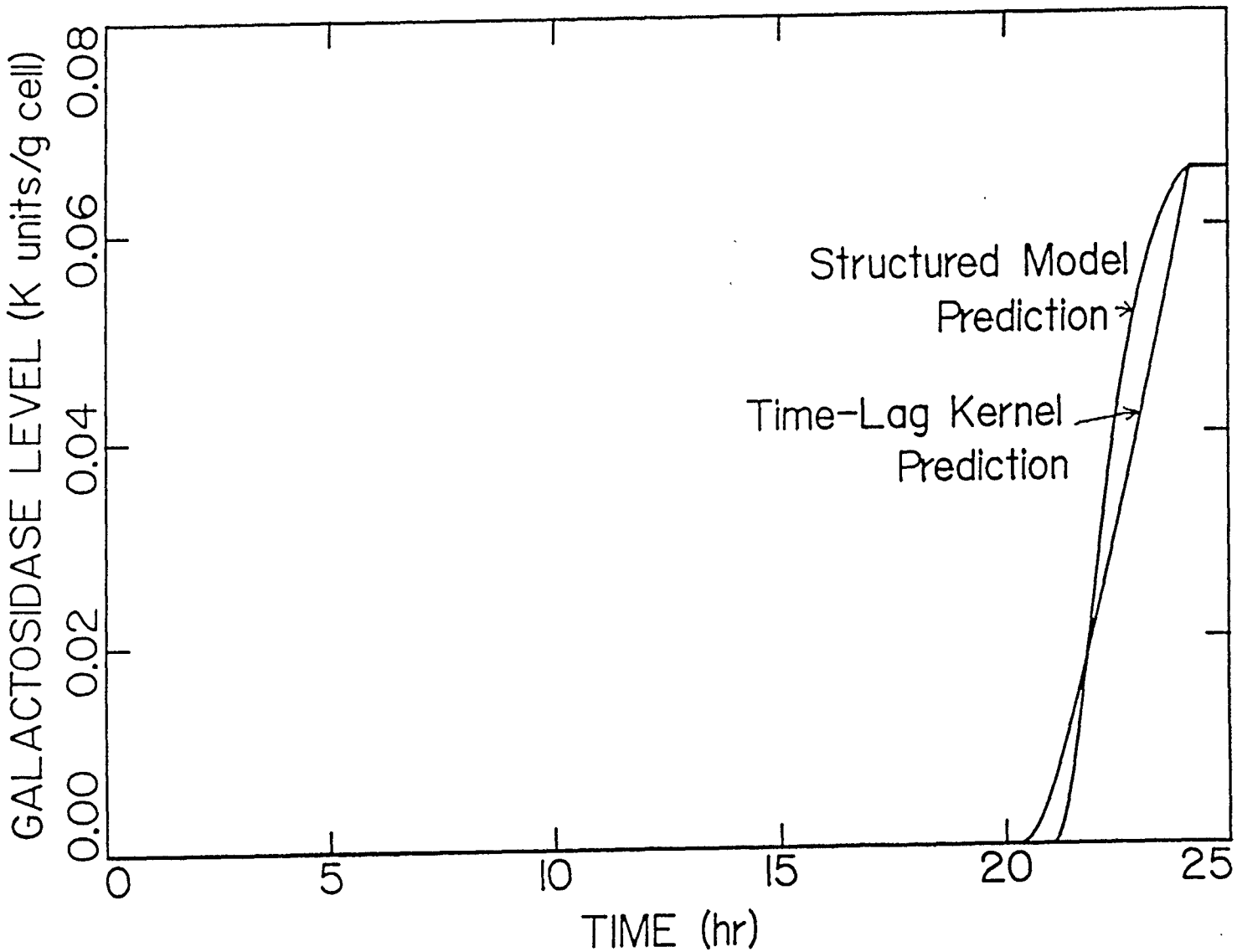

Figure 9. Comparison of the enzyme profiles calculated with Imanaka's structured model of enzyme production and the time-lag kernel for a batch fermentor.

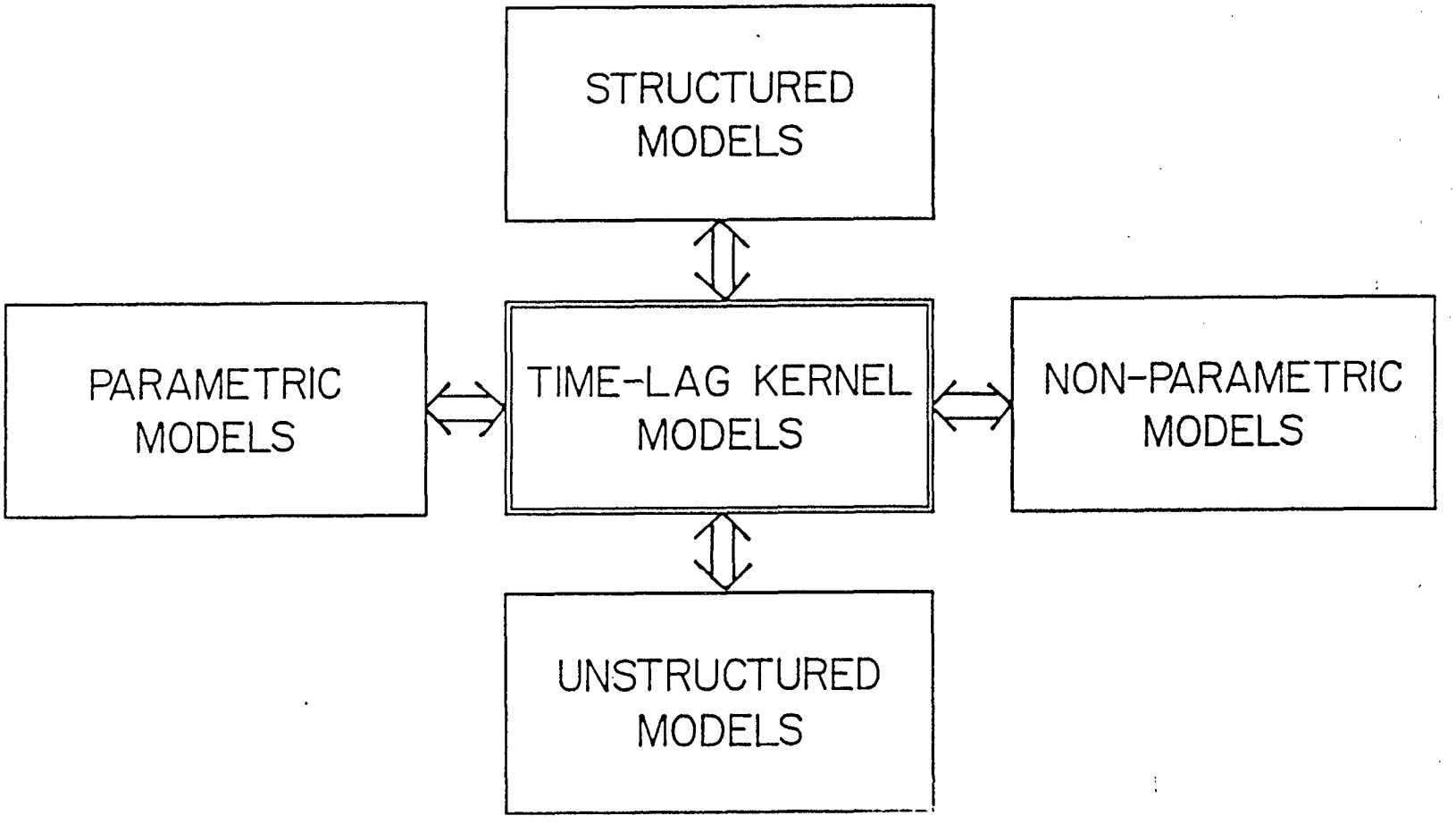

Figure 10. The kernel modeling approach is a hybrid of the parametric and non-parametric approaches. At the same time, it is also a hybrid of the structured and unstructured approaches.